Regulation of Interprotein Electron Transfer by Trp 191 of Cytochrome *c* Peroxidase†

Mark A. Miller,*,‡ Lidia Vitello,§ and James E. Erman§

Department of Chemistry and Biochemistry, University of California, San Diego, La Jolla, California 92093-0317, and Department of Chemistry, Northern Illinois University, DeKalb, Illinois 60115

Received April 20, 1995; Revised Manuscript Received July 5, 1995⊗

ABSTRACT: Cytochrome *c* peroxidase (CcP) reacts with peroxide to form compound I, an intermediate that has an oxy−ferryl iron center and a stable indolyl radical at Trp 191. During the normal catalytic cycle, the oxy−ferryl heme and the Trp 191 radical are reduced by sequential electron transfers from ferrous cytochrome *c* (Cc). To investigate the role of protein structure in these electron transfer reactions, mutagenesis was used to replace Trp 191 with Phe. The Trp 191 → Phe enzyme [CcP(MI,F191)] reacts with peroxide to form an oxy−ferryl iron center and a transient porphyrin radical. The reaction of Cc from horse and yeast with peroxide-oxidized CcP(MI,F191) was characterized under transient and steady-state conditions. The rate of ET from Cc to the oxy−ferryl heme of CcP(MI,F191) was decreased by at least 10 000-fold relative to the CcP(MI) parent. This effect was observed at 20 and 100 mM ionic strength, with both yeast and horse cytochrome *c* as the substrate. Thus, Trp 191 is a critical component of all pathways that permit rapid reduction of the oxy−ferryl heme by Cc under these conditions. The reaction of the porphyrin radical with Cc was difficult to characterize, owing to the short half-life of this intermediate. The oxidation of Cc by this intermediate had a maximum rate constant of 32 s^{-1} at pH 6.0, 25 °C. Circumstantial evidence suggests that the porphyrin radical is not directly reduced by Cc, but is instead reduced via a protein-based radical intermediate. The steady-state activity of the mutant enzyme was 300−600-fold lower than the CcP(MI) parent, but k_{cat} is 7−20 times greater than the rate constant for reduction of the oxy−ferryl heme under all conditions examined. Thus, the oxy−ferryl heme is not reduced to the ferric state under steady-state conditions. Transient changes in the absorption spectrum further indicate that steady-state oxidation of Cc^{2+} by CcP(MI,F191) occurs via reaction of peroxide with the oxy−ferryl enzyme.

Biological processes such as oxidative phosphorylation and photosynthesis depend upon efficient long-distance electron transfer (ET)[1] between redox centers embedded in a protein matrix. The protein matrix determines the rate and specificity of these reactions, but the structural basis for this control remains a matter of debate (Moser et al., 1992; Beratan et al., 1991; Freisner, 1994). The redox pair of cytochrome *c* peroxidase (CcP) and cytochrome *c* (Cc) provides a well-characterized physiological system for testing current models of interprotein ET. Crystal structures of both proteins are known individually (Finzel et al., 1984; Louie & Brayer, 1990), and structures of the noncovalent complexes formed between CcP and Cc from yeast (yCc) and horse (hCc) have also been reported (Pelletier & Kraut, 1992). The system is therefore well suited for testing the role of protein structure in determining ET rates.

The redox reaction catalyzed by CcP can be represented as shown in Scheme 1.

Scheme 1

$$CcP^{3+} + HOOH \rightleftarrows CcP^{4+}{=}O;Trp\ 191^{\bullet+} + H_2O \quad (1)$$

$$CcP^{4+}{=}O;Trp\ 191^{\bullet+} + Cc^{2+} \rightleftarrows CcP^{4+}{=}O;Trp\ 191^{\bullet+}{-}Cc^{2+} \quad (2)$$

$$CcP^{4+}{=}O;Trp\ 191^{\bullet+}{-}Cc^{2+} \rightarrow \text{compound II}{-}Cc^{3+} \quad (3)$$

$$\text{compound II} + Cc^{2+} \rightleftarrows \text{compound II}{-}Cc^{2+} \quad (4)$$

$$\text{compound II}{-}Cc^{2+} \rightarrow CcP^{3+}{-}Cc^{3+} \quad (5)$$

CcP^{3+} reacts initially with peroxide to form the oxidized intermediate called compound I (eq 1). The two oxidizing equivalents of peroxide are retained by compound I at two sites: one site is the iron, which is converted from ferric to oxy−ferryl ($Fe^{4+}{=}O$) state, and the other is Trp 191, which undergoes one-electron oxidation to produce a stable indolyl cation radical (Trp $191^{\bullet+}$) (Scholes et al., 1989; Mauro et al., 1988; Erman et al., 1989; Sivaraja et al., 1989). One of the oxidized sites is then reduced by a molecule of Cc^{2+}, producing the intermediate compound II (eqs 2 and 3). The remaining oxidized site of compound II is then reduced by

† Supported by NSF Grant MCB 94-20845 to M.A.M. and NSF Grant 91-21414 to J.E.E. and L.V.

‡ University of California, San Diego.

§ Northern Illinois University.

⊗ Abstract published in *Advance ACS Abstracts,* September 1, 1995.

[1] Abbreviations: CcP, yeast cytochrome *c* peroxidase; CcP(MI), a cloned cytochrome *c* peroxidase expressed in *E. coli*, described in Fishel et al. (1987); CcP(MI,F191), a mutant of CcP(MI) with Trp 191 replaced by Phe; hCc and yCc, the cytochromes *c* from horse heart and bakers' yeast, respectively; heme oxidation states of CcP, CcP(MI) and Cc are indicated as superscripts; $CcP^{4+}{=}O;Trp191^{\bullet+}$, compound I, the product of the reaction between ferric CcP and peroxide; $Trp191^{\bullet+}$, the indolyl radical formed at Trp 191 of CcP; $por^{\bullet+}$, porphyrin cation radical; $R_x^{\bullet}$, protein-based radical at an unspecified residue; ET, electron transfer; SDS−PAGE, sodium dodecyl sulfate−polyacrylamide gel electrophoresis.

0006-2960/95/0434-12048$09.00/0

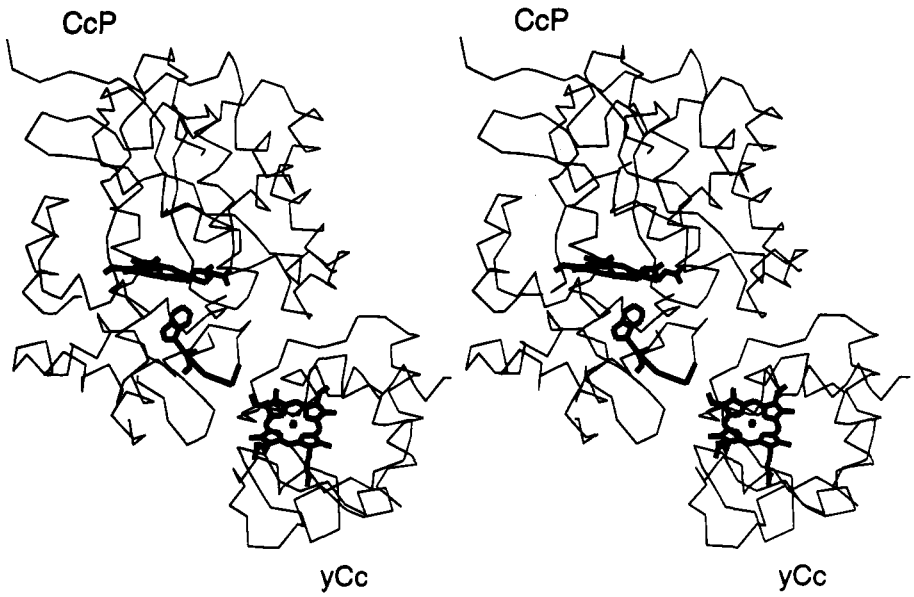

FIGURE 1: Stereo ribbon representation of the crystalline CcP(MI)−yCc complex. The α-carbon traces of CcP(MI) and Cc are delineated with thin lines. The two hemes and the electron transfer pathway proposed by Pelletier and Kraut (1992), including Trp 191 and the peptide backbone of residues 191−193, are delineated with bold lines.

Cc^{2+} to regenerate CcP^{3+} (eqs 4 and 5). Compound I reduction by Cc^{2+} is rapid, although the heme edges are separated by at least 17 Å within the CcP−Cc complex (Finzel et al., 1984; Pelletier & Kraut, 1992). The structure of the crystalline CcP−yCc complex and a putative ET pathway are shown in Figure 1.

The detailed mechanism of compound I reduction remains unclear. Two unresolved issues are as follows: (1) Which of the two sites is reduced first? (2) Is the mechanism ordered, or can the two sites be reduced independently? When Ru derivatives of hCc and yCc are employed at low ionic strength (Geren et al., 1991; Hahm et al., 1992, 1993), the data support an ordered mechanism, where the Trp 191 radical is reduced initially, and reduction of the oxy−ferryl heme as shown in Scheme 2.

Scheme 2

$$CcP^{4+}{=}O;\text{Trp } 191^{\bullet+} + Cc^{2+} \rightarrow CcP^{4+}{=}O + Cc^{3+} \quad (6)$$

$$CcP^{4+}{=}O + 2H^{+} \rightleftarrows CcP^{3+};\text{Trp } 191^{\bullet+} + H_2O \quad (7)$$

$$CcP^{3+};\text{Trp } 191^{\bullet+} + Cc^{2+} \rightleftarrows CcP^{3+};\text{Trp } 191^{\bullet+}{-}Cc^{2+} \quad (8)$$

$$CcP^{3+};\text{Trp } 191^{\bullet+}{-}Cc^{2+} \rightarrow CcP^{3+}{-}Cc^{3+} \quad (9)$$

In eq 6, Cc^{2+} reduces the Trp 191 radical, producing the oxy−ferryl enzyme. Equilibrium between the oxy−ferryl heme and the Trp 191 indole ring then creates an intermediate with a ferric iron center and a radical at Trp 191 (eq 7). The Trp 191 radical produced by this equilibrium is then reduced by electron transfer from Cc^{2+}, regenerating the resting ferric enzyme (eqs 8 and 9). The order of the reaction is reversed, however, in stopped-flow studies using native hCc and yCc at low ionic strength (Nuevo et al., 1993; Summers & Erman, 1988; Matthis et al., 1995). Under these conditions, the oxy−ferryl iron is reduced initially, and reduction of the Trp 191 radical follows. A common feature of the ordered mechanisms is that both predict an equilibrium between the two oxidized sites. Others have argued that the two sites can be reduced independently (Hazzard & Tollin, 1991; Kang et al., 1977). An independent reduction mechanism would be consistent with recent evidence that CcP has two binding sites for Cc (Mauk et al., 1994) and with evidence obtained using CcP and hCc substituted with a nonphysiological Zn−heme (Zhou & Hoffman, 1994; Stemp & Hoffman, 1993). No compelling evidence for independent reduction of the two sites has yet been presented, however.

In the present work, mutagenesis was used to simplify the mechanism of the ET reaction, by creating a CcP mutant that lacks one of the stable oxidized sites of compound I. The mutation of Trp 191 to Phe eliminates the site of the stable compound I radical, but does not alter the stability of the oxy−ferryl heme (Scholes et al., 1989; Mauro et al., 1988; Erman et al., 1989). Preliminary experiments indicated that the rate of ET from Cc^{2+} to the oxy−ferryl heme was decreased significantly by this mutation (Mauro et al., 1988). A detailed characterization of the ET reactions of the CcP(MI,F191) mutant is reported here.

MATERIALS AND METHODS

Materials. Horse heart (Type VI) and bakers' yeast iso-1 cytochromes *c* were obtained from Sigma and were used without further purification. Plasmid encoded CcP(MI) and CcP(MI,F191) were isolated from *Escherichia coli* strain SK383 and purified as described previously (Fishel et al., 1987). Concentrations of these enzymes were determined from their extinction coefficients at convenient absorption maxima: CcP(MI), $\epsilon_{408} = 102\ mM^{-1}\ cm^{-1}$; CcP(MI,F191), $\epsilon_{409} = 110\ mM^{-1}\ cm^{-1}$; hCc^{2+} and yCc^{2+}, $\epsilon_{550} = 27.8\ mM^{-1}\ cm^{-1}$. Hydrogen peroxide was standardized with cerium(III) sulfate (Koltoff et al., 1957). Transient kinetic studies were performed using a Hi-Tech Scientific PQ/SF-53 stopped-flow spectrophotometer with a 1 cm observation path. Slower reactions, steady-state kinetics, and absorption spectra were recorded using a Perkin-Elmer Lambda 3B dual-beam spectrophotometer.

Absorption Spectra. Crystals of CcP(MI,F191) or CcP(MI) were dissolved in 0.2 mM potassium phosphate buffer, pH 6.0, and the enzyme stocks were diluted into the buffers of interest. Absorption spectra of oxy−ferryl enzymes were

obtained as follows: the enzymes were first converted to their respective Fe^{2+}−CO derivatives (Ho et al., 1983; Miller et al., 1992); the Fe^{2+}−CO enzymes were mixed with equimolar HOOH and placed 2 cm from the beam of a 250 W tungsten−halogen bulb for 10 s. The absorption spectrum was recorded during the ensuing 3 min. Oxy−ferryl enzymes were titrated with Cc^{2+} to confirm that the enzyme was oxidized by 1 equiv above the ferric state.

Transient Kinetic Studies. Stopped-flow reactant syringes, mixer, and observation chamber were thermostated at 25 °C with a circulating water bath. Reactions were observed by monitoring changes in absorbance at several wavelengths, usually 396, 417, 434, and 550 nm. Reactant concentrations varied between 0.2 and 1.0 μM for CcP(MI,F191), 0.2 and 130 μM for HOOH, and 0.9 and 40 μM for hCc^{2+}. Slower reactions were also monitored by manual mixing of reactants.

Steady-State Kinetics. Steady-state oxidation of Cc^{2+} was monitored at 550 nm as described previously (Fishel et al., 1987; Kim et al., 1990). Buffers were prepared with 8.2 mM KH_2PO_4 and were adjusted to the desired final ionic strength (20−100 mM) by the addition of 1 M KNO_3. The resulting solution was adjusted to pH 6.0 with KOH. Reactions were conducted in a final volume of 1 mL of buffer solution of the desired ionic strength, containing 0.08 pmol−4 nmol of enzyme, 1−80 μM Cc^{2+}, and 150 μM HOOH. Individual kinetic traces were fit to a single-exponential decay using a commercially available software package. v_0 was determined from the first derivative of the best-fit line at $t = 0$. The reported values of v_0 and k_{cat} have been corrected to account for the oxidation of 2 mol of Cc^{2+}/turnover [i.e., $v_0 = (^1/_2)(d[Cc^{3+}]/dt)$]. Linearity of the reaction with enzyme concentration was demonstrated for all conditions reported, typically using four enzyme concentrations for each reported rate. Uncatalyzed oxidation of Cc^{2+} was less than 10% of total oxidation under all conditions described.

Cross-Linking Experiments. Samples containing 10 nmol of CcP(MI) or CcP(MI,F191) were prepared in 0.1 M potassium phosphate buffer, pH 6.0, and were then converted to compound I or Fe^{4+}=O state by adding peroxide to the Fe^{3+}- or Fe^{2+}−CO enzymes (Miller et al., 1992). A 10 μL aliquot of each sample was removed at the desired time, mixed with a reducing−denaturing gel loading buffer solution, and subjected to SDS−PAGE under reducing conditions as described previously (Fishel et al., 1987).

RESULTS

Oxidation of CcP(MI,F191)$^{3+}$ by Peroxide. The reaction of $CcP(MI,F191)^{3+}$ with peroxide produces an oxy−ferryl (Fe^{4+}=O) iron center and a transient porphyrin cation radical ($por^{\bullet+}$) (Erman et al., 1989). The progress of the reaction with peroxide was monitored at 396 nm, which is an isosbestic wavelength for the porphyrin cation radical and the oxy−ferryl heme. At this wavelength, the bimolecular reaction with peroxide is observed without interference from the oxidation and reduction of the porphyrin radical (Figure 2). The rate constant for this reaction has a linear dependence upon peroxide concentration, giving a bimolecular rate constant $k_1 = (1 \pm 0.4) \times 10^8$ M^{-1} s^{-1} at pH 6.0, 25 °C. When the same reaction is monitored at 406 nm, the absorbance shows a rapid decrease as the porphyrin radical is formed, followed by an increase as the radical is reduced by an internal electron donor (Figure 2). The rate of the

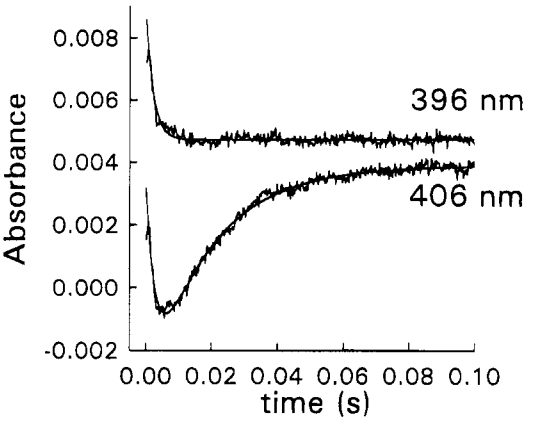

FIGURE 2: Reaction of CcP(MI,F191) with HOOH observed at 396 and 406 nm. The kinetic traces are arbitrarily displaced along the absorbance axis. Experimental conditions: [CcP(MI,F191)] = 0.47 μM; [HOOH] = 5.05 μM; in 20 mM ionic strength, pH 6.0, 25 °C. The trace at 396 nm was fit to a single-exponential decay using nonlinear regression analysis, giving a best-fit value of $k_{obs} = 360 \pm 40$ s^{-1}. The trace at 406 nm was fit with a sequential biexponential expression, giving best-fit rate constants of 450 ± 50 and 55 ± 4 s^{-1}.

second reaction is independent of peroxide concentration, and best fits of the data give a unimolecular rate constant $k_2 = 55 \pm 8$ s^{-1}.

A minimal mechanism for the reaction of ferric CcP(MI,F191) with peroxide is shown in Scheme 3.

Scheme 3

$$CcP(MI,F191)^{3+} + HOOH \xrightarrow{k_1} CcP(MI,F191)^{4+}{=}O;por^{\bullet+} + H_2O \quad (10)$$

$$CcP(MI,F191)^{4+}{=}O;por^{\bullet+} \xrightarrow{k_2} CcP(MI,F191)^{4+}{=}O;R_x^{\bullet} \quad (11)$$

The porphyrin radical ($por^{\bullet+}$) formed by the bimolecular reaction with peroxide (eq 10) is reduced via reaction with one or more protein residues, $R_x^{\bullet}$ (eq 11). The subscript x indicates that more than one amino acid residue may be oxidized.

Following the reduction of the porphyrin by an internal electron donor, the product has absorption maxima at 530 and 560 nm, indicating the presence of the oxy−ferryl heme (Figure 3A). Although the Soret and visible maxima of the $CcP(MI,F191)^{4+}$=O enzyme are quite similar to those of $CcP(MI)^{4+}$=O, the absorptivity of the mutant enzyme is significantly lower than the parent in the region from 600 to 635 nm (Figure 3A). The difference spectrum (Figure 3B) shows that the absorptivity of $CcP(MI,F191)^{4+}$=O is lower than that of $CcP(MI)^{4+}$=O in three regions.. The strongest peak in the difference spectrum appears at 608 nm and has a molar extinction coefficient $\epsilon = 2.2 \pm 0.2$ mM^{-1} cm^{-1}. Two other peaks are centered at 551 and 511 nm. It is not possible to determine with certainty whether the maxima observed in the difference spectrum are caused by the loss of one or more bands from the absorption spectrum or by a loss of intensity of several bands in this region.

It is important to establish whether or not the change in the absorption spectrum of the mutant enzyme is caused by oxidation of the porphyrin and its subsequent reduction by an internal donor. To examine this possibility, the $CcP(MI,F191)^{4+}$=O enzyme was prepared by the reaction of the

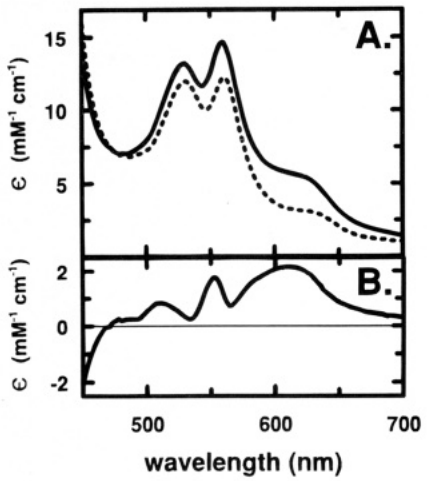

FIGURE 3: Absorption spectrum of the CcP(MI,F191)$^{3+}$ + peroxide reaction product. (A) Dashed line: Absolute absorption spectrum of CcP(MI,F191)$^{4+}$=O prepared by mixing CcP(MI,F191)$^{3+}$ with equimolar peroxide in 100 mM phosphate buffer, pH 6.0, 25 °C. Solid line: Absolute absorption spectrum of CcP(MI)$^{4+}$=O prepared by reaction of the ferrous enzyme with equimolar peroxide as described under Materials and Methods. (B) Difference absorption spectrum for CcP(MI)$^{4+}$=O−CcP(MI,F191)$^{4+}$=O.

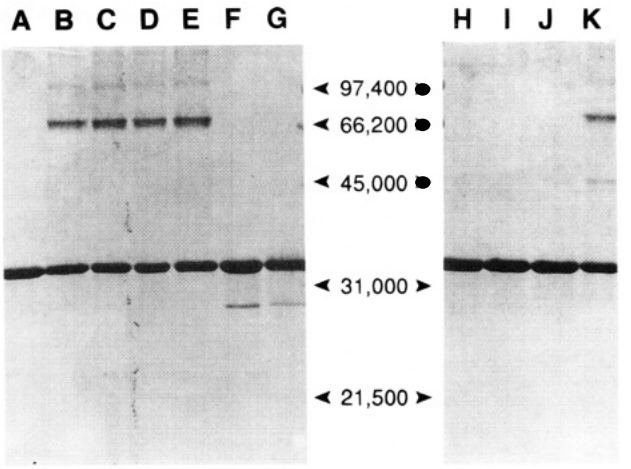

FIGURE 4: SDS−PAGE of the products of the reaction between CcP(MI,F191)$^{3+}$ and HOOH. Solutions containing 10 μM CcP(MI,F191) under various conditions were mixed with equimolar HOOH, and a small aliquot of the resulting solution (a volume containing ~34 μg of enzyme) was loaded into a well of a reducing SDS-acrylamide gel. Lane A, no HOOH; lane B, +HOOH, after 10 min; lane C, +HOOH, after 30 min; lane D, +HOOH, after 60 min; lane E, +HOOH, after 120 min; lane F, CcP(MI,F191)$^{2+}$, no addition; lane G, CcP(MI,F191)$^{2+}$ +HOOH after 10 mn; lane H, CcP(MI,F191)$^{3+}$, no addition; lane I, CcP(MI,F191)$^{3+}$ + 10 μM Cc^{2+}; lane J, CcP(MI,F191)$^{3+}$ + HOOH + 10 μM Cc^{2+}; lane K, CcP(MI,F191)$^{3+}$ + HOOH + 10 μM Cc^{3+}. The minor bands in lanes F and G are proteolytic fragments of CcP(MI,F191) that occasionally appear in the enzyme preparation. The presence or absence of the contaminant did not alter the results. Kinetic experiments were not conducted with enzyme containing this contaminant.

ferrous enzyme with equimolar peroxide (Ho et al., 1983). The absorption spectrum of this product is indistinguishable from that produced by the reaction of the ferric enzyme with peroxide, indicating that the change in the spectrum of the oxy−ferryl enzyme is not caused by oxidative destruction of a heme-linked residue.

Radical-Mediated Cross-Linking. The mechanism shown in Scheme 2 predicts that when the CcP(MI,F191)$^{3+}$ enzyme reacts with peroxide, one or more residues will be transiently oxidized to form a protein-based free radical. Previous work has shown that when protein-based radicals are produced by the reaction of peroxide with metmyoglobin, the radicals react to form myoglobin dimers that are linked through dityrosine (Tew & Ortiz de Montellano, 1988). Experiments were conducted to determine whether a similar cross-linking reaction accompanies the reaction of CcP(MI,F191)$^{3+}$ with peroxide. CcP(MI,F191)$^{3+}$ was mixed with equimolar peroxide, and the products of this reaction were analyzed by SDS−PAGE under reducing conditions. As shown in Figure 4, lane B, ~30% of the monomeric enzyme is converted to higher molecular weight material by this treatment. Most of the higher molecular weight material appears as a single band with a molecular mass of ~69 kDa, consistent with the formation of covalently linked homodimers of CcP(MI,F191). The amount of this product did not increase as the time of incubation increased from 10 to 60 min (Figure 4, lanes B−E). No cross-linking is observed when CcP(MI,F191)$^{4+}$=O was prepared by the reaction of the ferrous enzyme with peroxide (Figure 4, lanes F and G), further indicating that the cross-linking reaction depends upon transient porphyrin oxidation. The reaction is presumed to represent a radical-mediated dimerization (eq 12)

$$2\text{CcP(MI,F191)}^{4+}\text{=O;R}_x^{\bullet} \rightarrow [\text{CcP(MI,F191)}^{4+}\text{=O;R}_x]_2 \quad (12)$$

The results identify at least three oxidized intermediates that are formed by the reaction of CcP(MI,F191)$^{3+}$ with peroxide. The first is a transient porphyrin radical, which has a half-life of 14 ms under the present conditions. The second is a protein-based radical, formed when one (or more) amino acid side chains are oxidized by the porphyrin radical. This intermediate seems to persist under the present conditions for up to 10 min. A transient Tyr radical was observed in this time frame by EPR/ENDOR studies of CcP(MI,F191) (Scholes et al., 1989; Fishel et al., 1991). The third intermediate is the oxy−ferryl iron center, which has a half-life of ~2 h in the absence of added reductant. Experiments were conducted to determine the rate of ET from Cc^{2+} to each of these intermediates.

ET from Cc^{2+} to CcP(MI,F191)$^{4+}$=O. The stability of the CcP(MI,F191)$^{4+}$=O intermediate made it possible to measure ET from Cc^{2+} to the oxy−ferryl heme directly. To ensure that measurements of the intermolecular ET rate are meaningful, it is important to prevent the extensive intermolecular cross-linking and other oxidative damage that occurs when CcP(MI,F191)$^{3+}$ is mixed with equimolar peroxide. As shown in Figure 4, lanes I and J, the cross-linking reaction is eliminated when peroxide is added to CcP(MI,F191)$^{3+}$ in the presence of hCc^{2+}. This suggests that Cc^{2+} reduces a reactive intermediate prior to the formation of covalent cross-linkages. Consistent with this notion, addition of hCc^{3+} in place of hCc^{2+} does not prevent cross-linking. Instead, a new band with an apparent molecular mass of 45 kDa is observed along with the 69 kDa product, suggesting that a covalent CcP(MI,F191)−hCc^{3+} heterodimer is formed in addition to the homodimers of CcP(MI,F191).

Since cross-linking of CcP(MI,F191)$^{3+}$ is prevented by Cc^{2+}, all subsequent kinetic measurements of CcP(MI,F191)$^{4+}$=O reduction were made by adding stoichiometric amounts of HOOH to a solution containing CcP(MI,F191)$^{3+}$ and excess Cc^{2+}. Changes in the oxidation state of CcP(MI,F191) were monitored at 434 nm, the isosbestic point

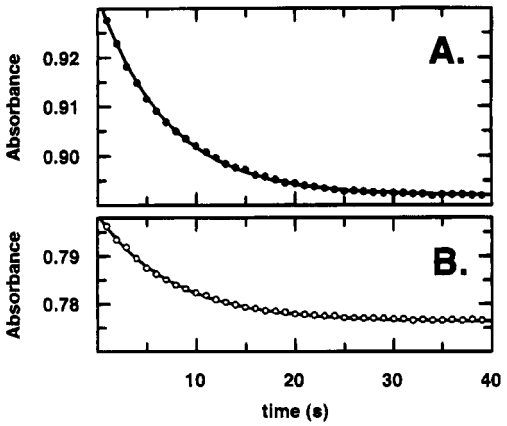

FIGURE 5: Reduction of CcP(MI,F191)$^{4+}$=O by Cc^{2+}. A 2 nmol sample of HOOH was added to a solution containing 2 nmol of CcP(MI,F191)$^{3+}$ and 30 nmol of yCc^{2+} in 1 mL of potassium phosphate + potassium nitrate buffer, ionic strength 100 mM, pH 6.0, 25 °C. Changes in absorbance were monitored at 550 (A) and 434 nm (B) and were fitted to a single-exponential decay. The solid line in (A) corresponds to k_{obs} = 0.142 s^{-1}, and a change in absorbance of 0.040 absorbance unit, which corresponds to oxidation of 2.05 nmol of Cc^{2+}. The solid line in (B) corresponds to k_{obs} = 0.133 s^{-1}.

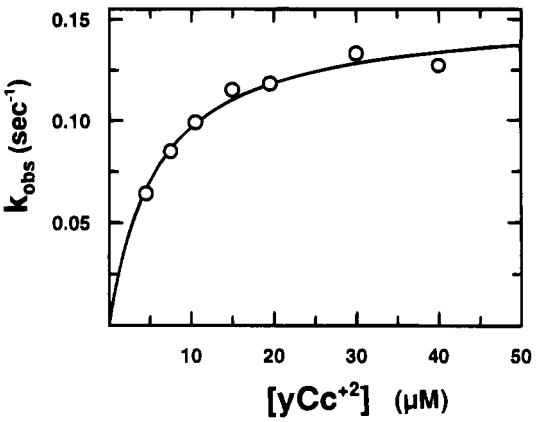

FIGURE 6: Dependence of the rate of CcP(MI,F191)$^{4+}$=O reduction on yCc^{2+} concentration. Conditions were as described in the legend to Figure 5, except that enzyme concentrations were varied to maintain pseudo-first-order conditions with respect to yCc^{2+}. The solid line represents the best fit of the points to the mechanism proposed in Scheme 4, where k_5 = 0.153 s^{-1} and K_B = 5.8 μM.

for Cc^{2+}/Cc^{3+}. Oxidation of Cc^{2+} was monitored at 550 nm, where changes in absorbance arising from CcP(MI,F191) oxidation are minimal. The addition of peroxide causes an immediate increase in absorbance at 434 nm, indicating that CcP(MI,F191)$^{3+}$ is converted to the oxy−ferryl state. The addition of peroxide also causes an immediate decrease in the absorbance at 550 nm. The magnitude of the initial decrease in absorbance corresponds to oxidation of 1.2 ± 0.1 mol of yCc^{2+} oxidized/mol of HOOH added. After the initial rapid decrease in absorbance at 550 nm, the absorbance continues to decrease slowly for up to several minutes (Figure 5A), depending upon the Cc^{2+} concentration. The decrease in absorbance at 550 nm is accompanied by a parallel decrease in absorbance at 434 nm (Figure 5B), indicating that CcP(MI,F191)$^{4+}$=O is reduced to the ferric state by Cc^{2+} during this slow phase of the reaction.

At both 434 and 550 nm, the decrease in absorbance is well fit by a single-exponential function, giving a rate constant (k_{obs}) that is independent of wavelength. The rate constant is independent of enzyme concentration, but has a hyperbolic dependence on Cc^{2+} concentration (Figure 6). The results are consistent with rapid equilibrium formation of a complex between CcP(MI,F191)$^{4+}$=O and Cc^{2+}, followed by ET, as shown in Scheme 4.

Scheme 4

$$\text{CcP(MI,F191)}^{4+}\text{=O} + \text{Cc}^{2+} \overset{K_B}{\rightleftharpoons} \text{CcP(MI,F191)}^{4+}\text{=O–Cc}^{2+} \quad (13)$$

$$\text{CcP(MI,F191)}^{4+}\text{=O–Cc}^{2+} + 2\text{H}^{+} \xrightarrow{k_5} \text{CcP(MI,F191)}^{3+}\text{–Cc}^{3+} + \text{H}_2\text{O} \quad (14)$$

The subscripts for rate and equilibrium constants are assigned to be consistent with the overall reaction mechanism proposed in Scheme 5 below. The values for K_B (the dissociation constant for the complex) and k_5 (the limiting rate of electron transfer) were determined for both hCc^{2+} and yCc^{2+} at 20 and 100 mM ionic strength (Table 1). The value of k_5 did not vary significantly with ionic strength for yCc^{2+} or hCc^{2+}. This is in contrast to previous reports that the rate of reduction of oxy−ferryl CcP increases as the ionic strength is increased (Nuevo et al., 1993; Hazzard et al., 1988). The value for K_B increases with increasing ionic strength for both hCc^{2+} and yCc^{2+}, as has been reported previously for the CcP(MI) parent (Liu et al., 1994). At 100 mM ionic strength, k_5 has a linear dependence upon Cc^{2+} up to 100 μM Cc^{2+}. K_B must be greater than 170 μM to account for the data at this ionic strength.

Table 1: Kinetic Parameters for ET from Cc^{2+} to CcP(MI,F191)$^{4+}$=O[a]

	ionic strength (mM)	k_5 (s^{-1})	K_B (μM)
yCc^{2+}	20	0.12 ± 0.01	2 ± 1
	100	0.153 ± 0.005	5.8 ± 0.7
hCc^{2+}	20	0.028 ± 0.002	10 ± 1
	50	0.020 ± 0.001	31 ± 4
	100	nd[b]	>100[b]

[a] Data were acquired in potassium phosphate + potassium nitrate buffers, pH 6.0, 25 °C. [b] nd, not determined. The dependence on hCc concentration was linear up to 100 μM, giving a bimolecular rate constant k_5 = (1.01 ± 0.07) × 10^2 M^{-1} s^{-1} for this reaction.

The amplitude of the slow phase of Cc^{2+} oxidation was calculated by extrapolating the exponential fit for oxidation to t = 0. The absorbance change calculated for this phase represents oxidation of 1.07 ± 0.04 mol of Cc^{2+}/mol of added HOOH. Thus, the enzyme catalyzes the quantitative reduction of peroxide by Cc^{2+}: 1 equiv of peroxide is reduced in the form of a transient oxidized intermediate during the mixing time of the experiment; the second equivalent is retained by CcP(MI,F191) as the oxy−ferryl heme and reduced during the slow phase shown in Figure 5. Approximately 20% of the slow phase occurs during the initial mixing time of the experiment.

ET from Cc^{2+} to CcP(MI,F191)$^{4+}$=O; R_x•. Additional experiments were conducted to characterize the reaction of Cc^{2+} with the transient intermediates formed in the initial stages of the peroxide reaction. To characterize the reaction of Cc^{2+} with protein-based radicals formed during the peroxide reaction, equimolar CcP(MI,F191)$^{3+}$ and HOOH were combined in one syringe and a solution of Cc^{2+} was placed in a second syringe of a stopped-flow spectrophotometer. The contents of the two syringes were mixed, and the oxidation of Cc^{2+} was monitored at 417 nm. Under these

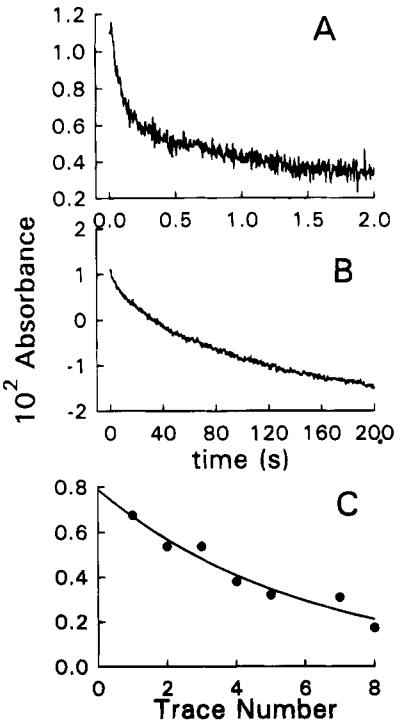

FIGURE 7: Reaction of peroxide-oxidized CcP(MI,F191)$^{3+}$ with hCc^{2+} monitored at 417 nm. Experimental conditions: 0.47 μM CcP(MI,F191) was mixed with equimolar HOOH immediately prior to the experiment. [hCc^{2+}] = 7.2 μM in (A) and (B) and 4.8 μM in (C); pH 6.0, 20 mM ionic strength buffer, 25 °C. (A) The fast phase of Cc^{2+} oxidation. Nonlinear regression gives best-fit values $k_3 = 10 \pm 1$ s^{-1} and 0.0064 absorbance unit for the amplitude. (B) The biphasic reaction observed at longer times. Nonlinear regression analysis gave $k_4 = 0.07 \pm 0.01$ s^{-1}, for the intermediate phase, which had an amplitude of 0.0049 absorbance unit, and $k_5 = 0.009 \pm 0.001$ s^{-1} for the slow phase, which had an amplitude of 0.0244 absorbance unit. (C) The decrease in amplitude of the fast reaction phase with the sequence number of the kinetic trace. CcP(MI,F191)$^{3+}$ and HOOH were mixed and placed in one syringe of the stopped-flow instrument, and the subsequent reaction with Cc^{2+} was monitored at 417 nm. The amplitude of the reaction is shown for each of eight subsequent traces, recorded at ~10 s intervals. The amplitude of the fast phase decreases with a half-life of ~35 s.

conditions, reduction of the porphyrin radical will be complete before the mixing experiment begins, and all Cc^{2+} oxidation can be attributed to reduction of the CcP(MI,F191)$^{4+}$=O; $R_x^{\bullet}$ intermediate(s) (eq 11), or a subsequent reaction product.

Typical results from such experiments are shown in Figure 7. Kinetic traces obtained at 417 nm showed that hCc^{2+} oxidation is complex, and at least three exponentials are required to adequately fit the absorbance changes. The fastest exponential phase is complete within 1 s (Figure 7A), while two subsequent phases occur on time scales from seconds to minutes (Figure 7B). The rate constants for the fast, intermediate, and slow phases are designated k_3, k_4, and k_5, to be consistent with Scheme 5 below.

The fastest exponential phase of hCc^{2+} oxidation is well separated from the slower phases, and the rate constant for this reaction could be determined accurately. The rate constant k_3 increases from 2 to 32 s^{-1} as the concentration of hCc^{2+} is increased from 1 to 31 μM. The amplitude of this reaction decreases as the time after mixing CcP(MI,F191)$^{3+}$ with peroxide increases, as expected for a reaction between hCc^{2+} and a transient intermediate. The half-time for the decrease in amplitude is ~35 s (Figure 7C), corresponding to a rate constant $k_6 = 0.02$ s^{-1} for decay of this intermediate. From the total amplitude of this phase, it was calculated that ~0.55 mol of hCc^{2+} is oxidized per mole of CcP(MI,F191) in the reaction mixture. That is, ~55% of the oxidized CcP(MI,F191) enzyme is reduced during this phase.

Oxidation of Cc^{2+} by peroxide-oxidized CcP(MI,F191) is quantitative under these conditions; therefore, the fraction of the oxidized enzyme that is not reduced during the fast phase of the reaction (~45% of the total) must be reduced by another process. It is likely that this reduction occurs during the intermediate phase of the reaction. Characterization of the intermediate phase is difficult because it is not well separated from the slowest process. The rate constant for the intermediate phase (k_4) ranges from 0.026 to 0.35 s^{-1} as the hCc^{2+} concentration increases from 1 to 31 μM. The amplitude of this phase corresponds to reduction of ~42% of the oxidized CcP(MI,F191) (Figure 7B), which would be consistent with the presence of a second intermediate, CcP(MI,F191)$^{4+}$=O; $R_2^{\bullet}$, that reacts more slowly with hCc^{2+}.

The slowest phase (k_5) of this reaction occurs in the same time regime as reduction of the oxy−ferryl enzyme (see above) and is accompanied by a decrease in absorbance at 434 nm. This process therefore corresponds to reduction of the oxy−ferryl iron center by hCc^{2+}.

ET from Cc^{2+} to CcP(MI,F191)$^{4+}$=O; por$^{\bullet+}$. To determine whether or not Cc^{2+} can reduce the porphyrin radical directly, a solution containing peroxide was mixed with a solution containing CcP(MI,F191)$^{3+}$ and hCc^{2+}, using the stopped-flow spectrophotometer. To maximize the fraction of CcP(MI,F191) present as the CcP(MI,F191)$^{4+}$=O, por$^{\bullet+}$ intermediate, HOOH concentrations from 5 to 145 μM were used. At these concentrations, the rate of porphyrin oxidation is 10−260 times greater than the rate of reduction of the porphyrin radical, and at least 75% of the enzyme will be in the porphyrin radical form when the peroxide reaction is completed.

A typical result from this type of experiment is shown in Figure 8. A rapid exponential phase of hCc^{2+} oxidation is observed initially (Figure 8A), followed by additional hCc^{2+} oxidation on a much slower time scale (Figure 8B). At least three exponentials must be assumed to obtain a satisfactory fit to the data. The fast, intermediate and slow phases are designated k_A, k_B, and k_C.

Only the fast phase of the reaction (k_A) occurs during the lifetime of the porphyrin radical. The rate constant for this phase of hCc^{2+} oxidation is independent of peroxide concentration (Figure 9A), but increases from 10 to 32 s^{-1} as the concentration of hCc^{2+} increases from 2 to 40 μM (Figure 9B). When fit to a model that assumed the rapid equilibrium formation of a CcP(MI,F191)−hCc^{2+} complex followed by electron transfer, the best fit of the data gives $k_A = 32 \pm 3$ s^{-1} for the limiting rate of electron transfer, and $K_1 = 4 \pm 1$ μM for equilibrium formation of the electron transfer complex. The change in absorbance at 550 nm indicates that 0.17 μM Cc^{2+} is oxidized during the fast reaction phase. The fast phase accounts for only 22% of the total oxidized CcP(MI,F191), assuming that one molecule of hCc^{2+} reacts with each molecule of CcP(MI,F191). A significant fraction of the oxidized enzyme must therefore be reduced by another pathway. This reduction may occur

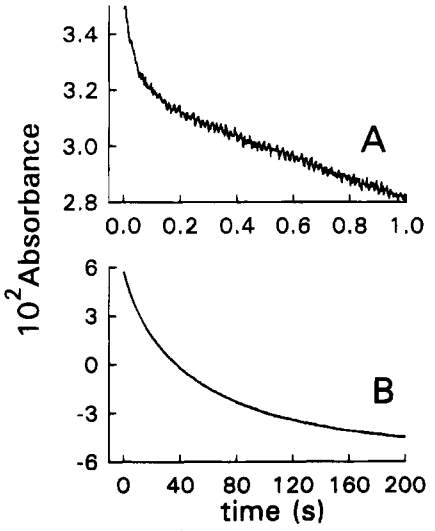

FIGURE 8: Oxidation of Cc^{2+} during the reaction of CcP(MI,F191)$^{3+}$ with excess HOOH. Experimental conditions: 0.77 μM CcP(MI,F191); 7.7 μM Cc^{2+}, + 7.5 μM HOOH, ionic strength 20 mM, pH 6.0, 25 °C. The reaction was monitored at 550 nm. (A) The fast phase of the reaction has a rate constant k_A = 20 s^{-1} superimposed upon a sloping baseline caused by the slower oxidation of Cc^{2+} by other processes. The amplitude of the fast phase was equivalent to 0.17 μM Cc^{2+} oxidized. (B) The slower phases of Cc^{2+} oxidation. The absorbance change was fit to a two-exponential equation with k_B and k_C equal to 0.07 and 0.013 s^{-1}, respectively. The absorbance changes correspond to oxidation of 1.5 and 4.0 μM Cc^{2+} in the k_B and k_C phases, respectively.

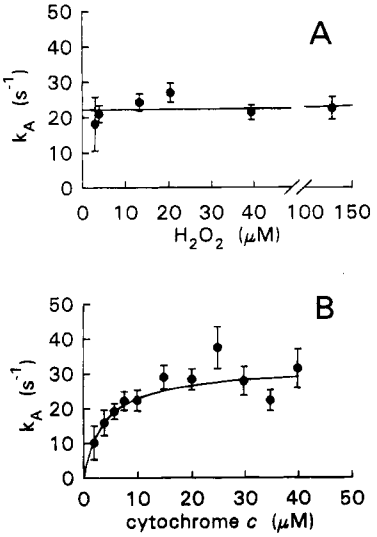

FIGURE 9: Concentration dependence of the rate constant k_A. Conditions were as stated in the legend to Figure 8, except that initial HOOH or Cc^{2+} concentrations were varied. (A) HOOH dependence of k_A. (B) Cc^{2+} dependence of k_A. Error bars represent ±1 standard deviation.

via ET from hCc^{2+} to subsequent intermediates or by side reactions between the protein-based radicals and the excess peroxide in the reaction mixture.

The intermediate phase of hCc^{2+} oxidation typically has a rate constant $k_B \approx 0.2$ s^{-1} under these conditions. This reaction is too slow to represent reduction of the porphyrin radical but is faster than the rate of reduction of the oxy−ferryl heme by hCc^{2+}. Evidence will be presented below that, during this phase, hCc^{2+} is oxidized by the reaction of peroxide with CcP(MI,F191)$^{4+}$=O.

The slowest phase occurred in the same time regime as the reduction of the oxy−ferryl heme, but the amplitude of this phase is much larger than that observed when equimolar peroxide and CcP(MI,F191)$^{3+}$ were mixed in the previous experiments. This phase apparently represents a catalytic process that is limited by the rate of reduction of the oxy−ferryl CcP(MI,F191) enzyme.

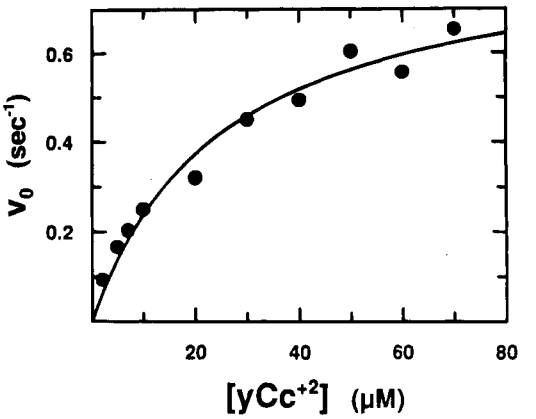

FIGURE 10: Dependence of initial rate of oxidation (v_0) on yCc^{2+} concentration for CcP(MI,F191). The initial rate was calculated as (nmol of Cc^{2+} oxidized)(s^{-1})(nmol of enzyme^{-1}), giving a final dimension of s^{-1}. Rate measurements were conducted in buffer of ionic strength 20 mM, as described under Materials and Methods.

Table 2: Steady-State Kinetic Parameters for Oxidation of Cc^{2+} by CcP(MI) and CcP(MI,F191)$^{4+}$=O[a]

	ionic strength (mM)	CcP(MI) k_{cat} (s^{-1})	CcP(MI) K_m (μM)	CcP(MI,F191) k_{cat} (s^{-1})	CcP(MI,F191) K_m (μM)
yCc^{2+}	20	461 ± 65	180 ± 33	0.85 ± 0.05	25 ± 5
	100	2168 ± 250	51 ± 12	3.15 ± 0.05	8.1 ± 0.6
hCc^{2+}	20	148 ± 4	1 ± 0.5	0.50 ± 0.01[b]	1.6 ± 0.4[b]
	100	151 ± 6	10 ± 1.5	0.37 ± 0.02	11 ± 2

[a] Determined in potassium phosphate + sodium chloride buffers, pH 6.0, 25 °C. [b] The data indicate that a second process also contributes to steady-state oxidation of Cc^{2+}. The process had a linear dependence on Cc^{2+} in the concentration range of the experiment, with k_{obs} = 8 ± 1 × 10^3 M^{-1} s^{-1}.

Steady-State Activity. The effect of the Trp 191 → Phe mutation on the steady-state oxidation of hCc^{2+} and yCc^{2+} was also examined. The rate of hCc^{2+} and yCc^{2+} oxidation by CcP(MI,F191) is not linear with time for more than a few seconds under the conditions employed here. Instead, the rate of Cc^{2+} oxidation decreased rapidly, and the change in absorbance at 550 nm could be modeled as a single-exponential decay. The initial rate of Cc^{2+} oxidation (v_0) was determined by fitting the change in absorbance to a single exponential function and taking the first derivative this function at t = 0. When determined in this way, v_0 is independent of enzyme concentration, but typically has a hyperbolic dependence on Cc^{2+} concentration. Representative data are shown in Figure 10. The values of k_{cat} and K_m for hCc^{2+} and yCc^{2+} are compared with those for the CcP(MI) parent in Table 2. Under all conditions, k_{cat} for CcP(MI,F191) is ~500-fold less than k_{cat} for CcP(MI), and the dependence of k_{cat} upon ionic strength and on the species of Cc employed is similar to the parent enzyme. The K_m for yCc^{2+} is ~6-fold less for the mutant enzyme than for the parental CcP(MI) at both 20 and 100 mM ionic strength. Like the parent enzyme [and like bakers' yeast CcP; Erman et al. (1991)], the K_m for yCc^{2+} *decreased* as the ionic strength *increased* from 20 to 100 mM. The K_m for hCc^{2+}

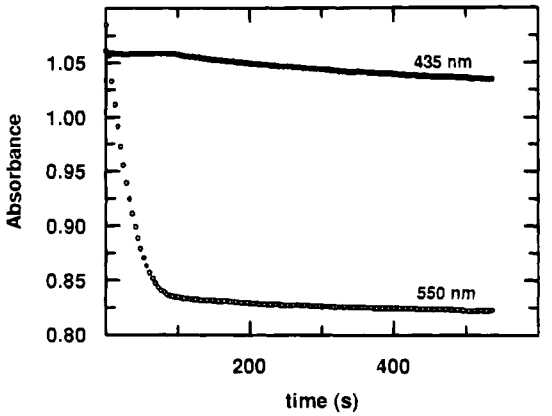

FIGURE 11: Wavelength dependence of the reaction of CcP(MI,F191) with hCc^{2+} in the presence of excess peroxide. HOOH (10 μM) was added to a mixture of 1 μM $CcP(MI,F191)^{3+}$ and 40 μM hCc^{2+}. Oxidation of hCc^{2+} was monitored at 550 nm (open circles), and reduction of $CcP(MI,F191)^{4+}$=O was monitored at 435 nm (solid circles).

is approximately the same for CcP(MI,F191) and the CcP(MI) parent at both 20 and 100 mM ionic strength, and increases with increasing ionic strength (Table 2), as reported for bakers' yeast CcP (Erman et al., 1991).

The value of k_{cat} for the CcP(MI,F191) mutant is 7–20-fold larger than the rate constant (k_5) for ET from Cc^{2+} to $CcP(MI,F191)^{4+}$=O in the same buffer (Tables 1 and 2). This indicates that ET from Cc^{2+} to oxy–ferryl CcP(MI,F191) does not occur under steady-state conditions. To establish the relationship between oxidation of Cc^{2+} under transient and steady-state conditions, a solution containing 1 μM $CcP(MI,F191)^{3+}$ and 40 μM hCc^{2+} was prepared, and HOOH was added to a final concentration of 10 μM. The change in absorbance was monitored immediately after peroxide addition at 550 nm and at 434 nm. At 550 nm, which monitors primarily Cc^{2+} oxidation, two distinct phases are observed: a rapid phase that is complete within 100 s and a slow phase that requires up to 10 min longer to complete (Figure 11). Based on the total change in absorbance at 550 nm, 2 mol of Cc^{2+} is oxidized per mole of HOOH added. Of this amount, ~19.1 μmol of Cc^{2+} is oxidized during the fast phase, and 0.9 μmol is oxidized during the slow phase. At 434 nm, which monitors changes in the oxidation state of CcP(MI,F191), no change in absorbance is seen during the time regime of the fast phase, and a decrease in absorbance is observed during the time regime of the slow phase (Figure 11). This indicates that the enzyme is in the oxy–ferryl state during the fast phase of Cc^{2+} oxidation and is reduced back to the ferric state during the slow phase. This conclusion is reinforced by subsequent experiments which showed that the amplitude of the fast phase increases in proportion to the amount of HOOH added, while the amplitude of the slow phase is proportional to the concentration of CcP(MI,F191). Thus, the overall reaction under steady-state conditions is

$$CcP(MI,F191)^{4+}{=}O + HOOH + 2Cc^{2+} + 2H^{+} \rightarrow CcP(MI,F191)^{4+}{=}O + 2Cc^{3+} + 2H_2O \quad (15)$$

The Trp 191 → Phe mutation impairs the ET rate so dramatically that the oxy–ferryl enzyme reacts more rapidly with HOOH than with Cc^{2+}.

DISCUSSION

The Trp 191 → Phe mutation eliminates the preferred pathway(s) for reduction of oxy–ferryl CcP(MI) by Cc^{2+}. The present work shows that ET from hCc^{2+} and yCc^{2+} to oxy–ferryl CcP(MI,F191) is 10^4–10^5-fold slower than that observed for the oxy–ferryl form of the CcP(MI) parent (Hazzard et al., 1987; Liu et al., 1994; Miller et al., 1988). The effect of the mutation cannot be correlated with global changes in the structure of the enzyme (Wang et al., 1990). It is unlikely that the driving force of the reaction is altered, since the midpoint potential for the Fe^{2+}/Fe^{3+} couple is not altered by the Trp 191 → Phe mutation (Mauro et al., 1988). The effect of the mutation is not caused by damage to the enzyme related to oxidation of the porphyrin, since the ET rate remains very slow when formation of the porphyrin radical is prevented by mixing the ferrous enzyme with peroxide. The evidence therefore indicates that rapid ET from Cc^{2+} to the oxy–ferryl heme is dependent upon an indole side chain at position 191.

The presence of Trp at position 191 is not sufficient to ensure rapid ET from Cc^{2+} to the oxy–ferryl heme, however. Mutation of Asp 235 to Asn decreases the ET rate and steady-state activity of CcP(MI) to levels comparable to CcP(MI,F191) without removing the indole ring [Ferrer et al. (1994); Miller, M. A., unpublished observations). Apparently, the effect of the Asp 235 to Asn mutation on ET is caused by perturbing the environment of the Trp 191 indole ring (Wang et al., 1990). The loss of the interaction between the Asp 235 carboxylate side chain and Trp 191-N_ϵ causes the Trp 191 indole side chain to rotate by 180° (Wang et al., 1990) and eliminates the stable compound I radical at Trp 191 (Fishel et al., 1991). Thus, the indole ring at position 191 must be readily oxidized and/or in a specific orientation to allow efficient ET between Cc^{2+} and the oxy–ferryl heme.

The basis for the dramatic effect of the Trp 191 → Phe mutation on the intermolecular ET reaction cannot be determined with certainty until the precise mechanism of compound I reduction has been determined. This aspect of ET in CcP remains ambiguous because of conflicting evidence about the rate of reduction of the radical site of I. When compound I reacts with photoreduced ruthenium-labeled yCc's, the rate of reduction of the Trp radical is much greater than 50 000 s^{-1} (Geren et al., 1991). On the other hand, stopped-flow studies suggest that reduction of the Trp 191 radical is too slow to occur during the steady-state reaction of the enzyme [less than 10 s^{-1} at 20 mM ionic strength; Matthis et al. (1995)]. These results are mutually exclusive, and it is not possible at this time to determine the basis for the discrepancy.

The effect of the Trp 191 → Phe mutation could be explained simply by assuming that, in the parent enzyme, ET occurs by an ordered mechanism, with the initial reduction occurring at the compound I radical. Reduction of the oxy–ferryl heme would follow, through equilibrium of the oxy–ferryl heme with the indole ring of Trp 191 (Geren et al., 1991; Hahm et al., 1992, 1993, 1994; Liu et al., 1994, 1995). An example of such a mechanism is presented in Scheme 2 above. The Trp 191 → Phe mutation (and the Asp 235 → Asn mutation) remove the readily oxidizable residue at position 191 and therefore would prevent reoxidation of the side chain at 191. This type of mechanism would accommodate a single binding site for

Cc^{2+}, and is consistent with the crystalline CcP–Cc complex, where Trp 191 is interposed between the hemes of Cc and CcP (Pelletier & Kraut, 1992).

There are potential difficulties with the mechanism proposed in Scheme 2. One problem is that the equilibrium between the Trp 191 radical and the oxy–ferryl heme appears to be too slow to account for the steady-state activity (Ho et al., 1983; Summers & Erman, 1988; Hazzard & Tollin, 1991; Liu et al., 1994). This problem can be reconciled with the data, however, if one assumes the existence of an intermediate that has not yet been detected. For example:

$$\underset{\text{compound I}}{CcP(MI)^{4+}{=}O} \rightleftarrows \underset{\text{compound II}}{CcP(MI)^{3+}{-}O^{-};Trp\ 191^{\bullet+}} +$$

$$2H^{+} \rightleftarrows \underset{\text{compound III}}{CcP(MI)^{3+};Trp\ 191^{\bullet+}} + H_2O$$

The intermediate compound I represents the oxy–ferryl enzyme, while compound II represents either a charge-transfer state or a true intermediate that is in rapid equilibrium with the oxy–ferryl enzyme. This intermediate can return to compound I or undergo conversion to compound III, which has a ferric heme and a radical at Trp 191. The characteristics of the reaction that have been described experimentally (Ho et al., 1983; Summers & Erman, 1988; Liu et al., 1994) can be explained by such a mechanism if (1) the equilibrium between compound I and compound II is rapid and favors compound I, (2) the formation of compound III is relatively slow and pH dependent, and (3) both compound II and compound III can react rapidly with Cc^{2+}. The proposed intermediate compound II is formed by electron transfer between two moieties that are in van der Waals contact, and so the equilibrium between compound I and compound II should be rapid. The equilibrium between compound I and compound III is comparatively slow because significant nuclear motion is required. The transition from compound I to compound III requires proton transfer to the coordinated oxygen ligand, movement of the oxygen ligand away from the heme, and movement of Arg 48 away from the heme ligand (Fulop et al., 1994). If compound II reacts rapidly with Cc^{2+}, the rapid reduction of the oxy–ferryl heme by Cc^{2+} required under steady-state conditions is possible despite the slow overall equilibrium between compound I and compound III. Whether or not such an intermediate exists remains to be determined.

A second problem with Scheme 2 is the evidence that Cc^{2+} can reduce the oxy–ferryl center directly at low ionic strength, as part of an ordered mechanism (Summers & Erman, 1988; Nuevo et al., 1993; Matthis & Erman, 1995; Matthis et al., 1995) or as part of a mechanism where the oxy–ferryl center and the Trp 191 radical are reduced independently at distinct binding sites (Hazzard & Tollin, 1991; Kang et al., 1977; Zhou & Hoffman, 1994; Stemp & Hoffman, 1993). If Cc^{2+} reduces the oxy–ferryl heme directly, the ET rate for the Trp 191 → Phe mutant should increase at low ionic strength, where this pathway becomes more important. No such increase is observed for hCc^{2+} or yCc^{2+}. Therefore, if a second pathway exists for reduction of the oxy–ferryl heme, it also depends upon Trp 191.

The effect of the Trp 191 → Phe mutation on the absorption spectrum of the oxy–ferryl enzyme (Figure 3) may cause the perturbation of this second pathway. Du et al. (1991) assigned the bands in the visible region of oxy–ferryl peroxidase primarily to porphyrin π–Fe=O ligand π^* transitions. The authors suggest that these bands are of sufficiently low energy to participate in the reduction of compound II by Cc^{2+}. If this is true, it is not unreasonable to suggest that the loss of a band in this region could impair a pathway for direct ET to the oxy–ferryl heme. It is interesting to note that the loss of absorptivity near 620 nm is seen only in mutations that severely impair ET to the oxy–ferryl heme [including several mutants at Trp 191, and the Asp 235 → Asn mutation; Vitello et al. (1992)]. No comparable effect has been seen for mutations at 30 or so other positions [Fishel et al. (1991); M. A. Miller, unpublished observations].

ET from Cc^{2+} to $CcP(MI,F191)^{4+}{=}O$; $por^{\bullet+}$. The data provide circumstantial evidence that the porphyrin radical is not reduced directly by Cc^{2+}. The limiting rate constant for ET to peroxide-oxidized CcP(MI,F191), 32 s^{-1}, is identical (within experimental error) to that for ET to the intermediate $CcP(MI,F191)^{4+}{=}O$; $R_1^{\bullet}$. This strongly suggests that both processes represent ET to a transient intermediate formed when an internal electron donor reduces the porphyrin radical. Moreover, it seems unlikely that the porphyrin radical could be reduced with a rate constant that is 10^3 faster than the rate for reduction of the oxy–ferryl center. While direct reduction of the porphyrin radical cannot yet be ruled out, the present results place an upper limit of 32 s^{-1} on the rate of ET from Cc^{2+} to the porphyrin radical, since this is the maximum rate of Cc^{2+} oxidation by the $CcP(MI,F191)^{4+}{=}O;\ por^{\bullet+}$ species. If direct reduction of the porphyrin occurs, it will compete with the reduction of the porphyrin by an internal electron donor (k_2 = 55 s^{-1}). The relative value of the two rate constants predicts that only 37% of the porphyrin radical species will be reduced by Cc^{2+}, while the remaining 63% will be reduced by an internal electron donor.

A minimal mechanism for the ET reactions of peroxide-oxidized CcP(MI,F191) with Cc^{2+} is shown in Scheme 5.

Scheme 5

$$CcP(MI,F191)^{3+} + HOOH \xrightarrow{k_1} CcP(MI,F191)^{4+}{=}O;por^{\bullet+} \quad (16)$$

$$CcP(MI,F191)^{4+}{=}O;por^{\bullet+} \xrightarrow{k_2} CcP(MI,F191)^{4+}{=}O;R_x^{\bullet} \quad (17)$$

$$CcP(MI,F191)^{4+}{=}O;R_x^{\bullet} + Cc^{2+} \overset{K_A}{\rightleftharpoons} CcP(MI,F191)^{4+}{=}O;R_x^{\bullet}{-}Cc^{2+} \quad (18)$$

$$CcP(MI,F191)^{4+}{=}O;R_x^{\bullet}{-}Cc^{2+} \xrightarrow{k_3} CcP(MI,F191)^{4+}{=}O{-}Cc^{3+} \quad (19)$$

$$CcP(MI,F191)^{4+}{=}O + Cc^{2+} \overset{K_B}{\rightleftharpoons} CcP(MI,F191)^{4+}{=}O{-}Cc^{2+} \quad (20)$$

$$CcP(MI,F191)^{4+}{=}O{-}Cc^{2+} \xrightarrow{k_5} CcP(MI,F191)^{3+}{-}Cc^{3+} \quad (21)$$

A porphyrin radical is created by the initial reaction with peroxide (eq 16). The porphyrin radical reacts with amino acid side chains of the enzyme to produce one or more protein-based radical species (eq 17). In the absence of Cc^{2+},

the reactive protein-based radical species produced in eq 17 disappears, and this oxidizing equivalent is dissipated through the formation of covalently linked dimers of CcP(MI,F191) (eq 12) and other uncharacterized products. In the presence of Cc^{2+}, the protein-based radical(s) is reduced through formation of a complex with Cc^{2+}, followed by electron transfer (eqs 18 and 19). The present work characterizes reduction of only one site ($k_3 = 32\ s^{-1}$; $K_a = 4\ \mu M$), although the results suggest that at least one other species ($k_4 = 0.35\ s^{-1}$) exists. It is possible that these two oxidized sites are formed independently or that reduction by Cc^{2+} competes with transfer of the oxidizing equivalent from one site to another. The presence of two kinetic phases during this reaction (Figure 7) requires that equilibration between the two sites is slow relative to the rate of reduction by Cc^{2+}. Finally, the oxy−ferryl heme is reduced via formation of an electron transfer complex between $CcP(MI,F191)^{4+}$=O and Cc^{2+} (eq 20) followed by ET, which returns the enzyme to the ferric state (eq 21).

Steady-State Activity. The results show that the oxy−ferryl heme is not reduced to the ferric state during steady-state catalysis by CcP(MI,F191). A minimal mechanism that is consistent with the data is given in Scheme 6.

Scheme 6

$$CcP(MI,F191)^{4+}{=}O + HOOH \rightarrow CcP(MI,F191)^{4+}{=}O;R_x^{\bullet},R_y^{\bullet} + 2\ H_2O \quad (22)$$

$$CcP(MI,F191)^{4+}{=}O;R_x^{\bullet},R_y^{\bullet} + Cc^{2+} + H^+ \rightarrow CcP(MI,F191)^{4+}{=}O;R_y^{\bullet} + Cc^{3+} \quad (23)$$

$$CcP(MI,F191)^{4+}{=}O;R_y^{\bullet} + Cc^{2+} + H^+ \rightarrow CcP(MI,F191)^{4+}{=}O + Cc^{3+} \quad (24)$$

In eq 22, peroxide reacts with the oxy−ferryl heme to generate an enzyme form that is oxidized by 2 equiv above the oxy−ferryl state. This intermediate then undergoes reaction with two molecules of Cc^{2+} to regenerate the oxy−ferryl enzyme (eqs 23 and 24).

The oxy−ferryl forms of other peroxidases are known to undergo reaction with HOOH to produce an $Fe^{2+}-O_2$ intermediate [compound III; Nakajima and Yamazaki (1987) and references therein]. While compound III can be produced by the CcP(MI,F191) enzyme under some conditions (Miller et al., 1992), it cannot be detected when $CcP(MI,F191)^{4+}$=O is mixed with excess peroxide (M. Miller, unpublished observation). Instead, a "hyper-oxidized" intermediate is formed that can be reduced stoichiometrically by Cc^{2+}. The intermediate suggested in eq 22 seems a likely possibility, based on the reactions of the enzyme described above. The results reported here are consistent with any mechanism where (1) the reaction of the oxy−ferryl enzyme with peroxide is rate-limiting or (2) the oxidizing equivalents are transferred rapidly from the heme to protein-based radicals, so that the heme remains in the oxy−ferryl state. The rapid decrease in steady-state activity with time may indicate that reduction by Cc^{2+} is not fast enough to prevent the destruction of the internal electron donor(s) by competing side reactions.

The steady-state activity of the CcP(MI,F191) enzyme is substantially lower than that of the CcP(MI) parent, but both enzymes exhibit a similar dependence on ionic strength and the species of origin of the Cc^{2+} substrate. With hCc^{2+} as the substrate, both CcP(MI,F191) and CcP(MI) have a constant value of k_{cat} at 20 and 100 mM ionic strength, and the apparent K_m increases as the ionic strength of the buffer increases. When yCc^{2+} is used as the substrate, the value of k_{cat} is greater at 100 mM ionic strength than at 20 mM ionic strength for both enzymes, and the K_m for yCc^{2+} increases as the ionic strength decreases. The increase in K_m at low ionic strength has recently been suggested to reflect the binding of yCc^{2+} at a second binding site (Mauk et al., 1994; Wang & Margoliash, 1995; Matthis & Erman, 1995). Apparently, this second binding site has a low affinity for yCc, and it becomes catalytically relevant only at fairly low ionic strength. The present results are consistent with this model, but clearly show that ET by both the high- and low-affinity sites requires the presence of Trp 191 for efficient function.

The results presented here demonstrate the ability of the CcP(MI,F191) mutant enzyme to catalyse steady-state oxidation of Cc^{2+} without reduction of the oxy−ferryl heme. Thus, steady-state activity cannot be assumed to measure the rate of reduction of the oxy−ferryl heme by Cc^{2+}. The report that second-site mutations at His 175 restore ET from Cc^{2+} to the heme of the Trp 191 → Phe enzyme must therefore be reevaluated, since these mutations have in fact been shown only to increase the steady-state activity (Choudhury et al., 1994). The present results indicate that second-site mutations may increase the steady-state activity of the Trp 191 → Phe enzyme by increasing the reactivity of the oxy−ferryl enzyme with peroxide or by increasing the reactivity of Cc^{2+} with the oxidized intermediate(s) produced when the oxy−ferryl enzyme reacts with peroxide. Conclusive evidence for reversal of the effect of the Trp 191 → Phe mutation must therefore await a direct evaluation of ET from Cc^{2+} to the oxy−ferryl heme of the double-mutant enzymes.

ACKNOWLEDGMENT

The authors are grateful to Sunny Kim for outstanding technical assistance.

REFERENCES

Beratan, D. N., Betts, J. N., & Onuchic, J. N. (1991) *Science 252*, 1285−1288.

Choudhury, K., Sundaramoorthy, M., Hickman, A., Yonetani, T., Woehl, E., & Poulos, T. L. (1994) *J. Biol. Chem. 269*, 20239−20249.

Du, P., Axe, F. U., Loew, G. H., Canuto, S., & Zerner, M. (1991) *J. Am. Chem. Soc. 113*, 8614−8621.

Erman, J. E., Vitello, L. B., Mauro, J. M., & Kraut, J. (1989) *Biochemistry 28*, 7992−7995.

Erman, J. E., Kang, D. S., Kim, K. L., Summers, F. E., & Vitello, L. B. (1991) *Mol. Cryst. Liq. Cryst. 194*, 253−258.

Ferrer, J. C., Turano, P., Banci, L., Bertini, I., Morris, I. K., Smith, K. M., Smith, M., & Mauk, A. G. (1994) *Biochemistry 33*, 7819−7829.

Finzel, B. C., Poulos, T. L., & Kraut, J. (1984) *J. Biol. Chem. 259*, 13027−13036.

Fishel, L. A., Villafranca, J. E., Mauro, J. M., & Kraut, J. (1987) *Biochemistry 26*, 351−360.

Fishel, L. A., Farnum, M. F., Mauro, J. M., Miller, M. A., Kraut, J., Liu, Y., Tan, X.-T., & Scholes, C. P. (1991) *Biochemistry 30*, 1986−1996.

Freisner, R. A. (1994) *Structure 2*, 339−343.

Fulop, V., Phizackerley, R. P., Soltis, S. M., Clifton, F. J., Wakatsuki, S., Erman, J., Hajdu, J., & Edwards, S. L. (1994) *Structure 2*, 201−208.
Geren, L., Hahm, S., Durham, B., & Millett, F. (1991) *Biochemistry 30*, 9450−9457.
Hahm, S., Durham, B., & Millett, F. (1992) *Biochemistry 30*, 3472−3477.
Hahm, S., Durham, B., & Millett, F. (1993) *J. Am. Chem. Soc. 115*, 3372−3373.
Hahm, S., Miller, M. A., Geren, L., Kraut, J., Durham, B., & Millett, F. (1994) *Biochemistry 33*, 1473−1480.
Hazzard, J. T., & Tollin G. (1991) *J. Am. Chem. Soc. 113*, 8956−8957.
Hazzard, J. T., Poulos, T. L., & Tollin, G. (1987) *Biochemistry 26*, 2836−2848.
Hazzard, J. T., McLendon, G., Cusanovich, M., Das, G., Sherman, F., & Tollin, G. (1988) *Biochemistry 27*, 4445−4451.
Ho, P. S., Hoffman, B. M., Kang, C. H., & Margoliash, E. (1983) *J. Biol. Chem. 258*, 4356−4363.
Kang, C. H., Ferguson-Miller, S., & Margoliash, E. (1977) *J. Biol. Chem. 252*, 919−926.
Kim, K. L., Kang, D. S., Vitello, L. B., & Erman, J. E. (1990) *Biochemistry 29*, 9150−9159.
Kolthoff, I. M., Belcher, R., Stenger, V. A., & Matsuyama, G. (1957) in *Volumetric Analysis* (Kolthoff, I. M., Ed.) Vol. III, pp 75−76, Interscience Publishers, New York.
Liu, R.-Q., Miller, M. A., Han, G. W., Hahm, S., Geren, L., Hibdon, S., Kraut J., Durham, B., & Millett, F. (1994) *Biochemistry 33*, 8678−8685.
Liu, R. Q., Hahm, S., Miller, M. A., Durham, B., & Millett, F. (1995) *Biochemistry 34*, 973−983.
Louie, G. V., & Brayer, G. D. (1990) *J. Mol. Biol. 214*, 527−555.
Marcus, R. A., & Sutin, N. (1985) *Biochim. Biophys. Acta 811*, 265−322.
Matthis, A., & Erman, J. E. (1995) *Biochemistry 34*, 9985−9990.
Matthis, A., Vitello, L. B., & Erman, J. E. (1995) *Biochemistry 34*, 9991−9999.
Mauk, M. R., Ferrer, J. C., & Mauk, A. G. (1994) *Biochemistry 33*, 12609−12614.
Mauro, J. M., Fishel, L. A., Hazzard, J. T., Meyer, T. E., Tollin, G., Cusanovich, M. A., & Kraut, J. (1988) *Biochemistry 27*, 6243−6256.
Miller, M. A., Hazzard, J. T., Mauro, J. M., Edwards, S. L., Simons, P. C., Tollin, G., & Kraut J. (1988) *Biochemistry 27*, 9081−9088.
Miller, M. A., Bandyopadhyay, D., Mauro, J. M., Traylor, T. G., & Kraut, J. (1992) *Biochemistry 31*, 2789−2797.
Moser, C. C., Keske, J. M., Warncke, K., Faird, R. S., & Dutton, P. L. (1992) *Nature 325*, 796−802.
Nakajima, R., & Yamazaki, I. (1987) *J. Biol. Chem. 262*, 2576−2581.
Nuevo, M. R., Chu, H.-H., Vitello, L., & Erman, J. E. (1993) *J. Am. Chem. Soc. 115*, 5873−5874.
Pelletier, H., & Kraut, J. (1992) *Science 258*, 1748−1755.
Scholes, C. P., Liu, Y., Fishel, L. A., Farnum, M. F., Mauro, J. M., & Kraut, J. (1989) *Isr. J. Chem. 29*, 85−92.
Sivaraja, M., Goodin, D. B., Smith, M., & Hoffman, B. M. (1989) *Science 245*, 738−740.
Stemp, E. A., & Hoffman, B. M. (1993) *Biochemistry 32*, 10848−10865.
Summers, F. E., & J. E. Erman (1988) *J. Biol. Chem. 263*, 14267−14275.
Tew, D., & Ortiz de Montellano, P. R. (1988) *J. Biol. Chem. 263*, 17880−17886.
Vitello, L. B., Erman, J. E., Miller, M. A., Mauro, J. M., & Kraut, J. (1992) *Biochemistry 31*, 11524−11535.
Wang, J., Mauro, J. M., Edwards, S. L., Oatley, S. J., Fishel, L. A., Ashford, V. A., Xuong, N.-h., & Kraut, J. (1990) *Biochemistry 29*, 7160−7173.
Wang, Y., & Margoliash, E. (1995) *Biochemistry* 34, 1948−1958.
Zhou, J., & Hoffman, B. M. (1994) *Science 265*, 1693−1696.

BI9508810